

See discussions, stats, and author profiles for this publication at: <https://www.researchgate.net/publication/256499545>

# Epoxide Pathways Improve Model Predictions of Isoprene Markers and Reveal Key Role of Acidity in Aerosol Formation

ARTICLE *in* ENVIRONMENTAL SCIENCE & TECHNOLOGY · SEPTEMBER 2013

Impact Factor: 5.33 · DOI: 10.1021/es402106h · Source: PubMed

CITATIONS

32

READS

85

16 AUTHORS, INCLUDING:



**Robert Pinder**

United States Environmental Protection Age...

74 PUBLICATIONS 1,682 CITATIONS

SEE PROFILE



**Shannon Capps**

University of Colorado Boulder

30 PUBLICATIONS 204 CITATIONS

SEE PROFILE



**John H Offenberg**

United States Environmental Protection Age...

102 PUBLICATIONS 4,375 CITATIONS

SEE PROFILE



**Tadeusz E Kleindienst**

United States Environmental Protection Age...

134 PUBLICATIONS 4,498 CITATIONS

SEE PROFILE

# Epoxide Pathways Improve Model Predictions of Isoprene Markers and Reveal Key Role of Acidity in Aerosol Formation

Havala O. T. Pye,<sup>\*,†</sup> Robert W. Pinder,<sup>†</sup> Ivan R. Piletic,<sup>†</sup> Ying Xie,<sup>†,‡</sup> Shannon L. Capps,<sup>†</sup> Ying-Hsuan Lin,<sup>¶</sup> Jason D. Surratt,<sup>¶</sup> Zhenfa Zhang,<sup>¶</sup> Avram Gold,<sup>¶</sup> Deborah J. Luecken,<sup>†</sup> William T. Hutzell,<sup>†</sup> Mohammed Jaoui,<sup>§</sup> John H. Offenberg,<sup>†</sup> Tadeusz E. Kleindienst,<sup>†</sup> Michael Lewandowski,<sup>†</sup> and Edward O. Edney<sup>†</sup>

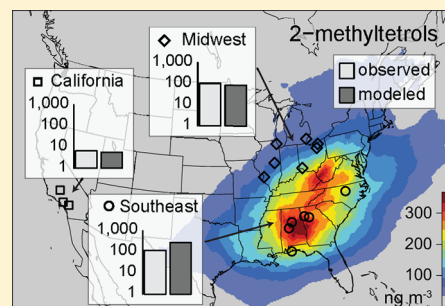
<sup>†</sup>National Exposure Research Laboratory, US Environmental Protection Agency, Research Triangle Park, North Carolina, 27711 United States

<sup>¶</sup>Department of Environmental Sciences and Engineering, University of North Carolina at Chapel Hill, North Carolina, 27599 United States

<sup>§</sup>Alion Science and Technology, Box 12313, Research Triangle Park, North Carolina, 27709 United States

## Supporting Information

**ABSTRACT:** Isoprene significantly contributes to organic aerosol in the southeastern United States where biogenic hydrocarbons mix with anthropogenic emissions. In this work, the Community Multiscale Air Quality model is updated to predict isoprene aerosol from epoxides produced under both high- and low- $\text{NO}_x$  conditions. The new aqueous aerosol pathways allow for explicit predictions of two key isoprene-derived species, 2-methyltetrols and 2-methylglyceric acid, that are more consistent with observations than estimates based on semivolatile partitioning. The new mechanism represents a significant source of organic carbon in the lower 2 km of the atmosphere and captures the abundance of 2-methyltetrols relative to organosulfates during the simulation period. For the parametrization considered here, a 25% reduction in  $\text{SO}_x$  emissions effectively reduces isoprene aerosol, while a similar reduction in  $\text{NO}_x$  leads to small increases in isoprene aerosol.



## INTRODUCTION

$\text{PM}_{2.5}$  (particles with aerodynamic diameters of  $2.5 \mu\text{m}$  or less) is a criteria pollutant with implications for public health and climate. Organic aerosol resulting from complex interactions of various emission sources significantly contributes to  $\text{PM}_{2.5}$ .<sup>1</sup> The spatial, seasonal, and temperature trends in aerosol optical thickness over the eastern United States indicate a significant role for biogenic secondary organic aerosol (SOA);<sup>2</sup> additionally, more than half of aerosol carbon is modern (vs fossil) in origin for a variety of locations,<sup>3,4</sup> which is consistent with a biogenic hydrocarbon source.

Isoprene, the most abundant non-methane hydrocarbon emitted,<sup>5</sup> is likely a large contributor to organic aerosol, particularly in the southeastern United States. Organic carbon (OC) model underestimates such as those in the Community Multiscale Air Quality (CMAQ) model<sup>6</sup> may arise from an underrepresentation of isoprene aerosol pathways. Isoprene-derived compounds detected in ambient aerosol, including 2-methyltetrols, 2-methylglyceric acid (2-MG), and organosulfates, account for 19.4% of organic aerosol in the work of Lin et al.<sup>7</sup> When adjusted to total OC using laboratory-based ratios, 12–29% of total OC is attributable to isoprene.<sup>8–10</sup> Methyltetrols are likely the most abundant individual isoprene SOA constituents and have been found to account for up to

6.6% of OC in Centreville, Alabama,<sup>11</sup> and 5.2–8.9% of total organic aerosol in Yorkville, Georgia.<sup>7</sup> Factors derived from positive matrix factorization (PMF) of aerosol mass spectrometer (AMS) data have been linked with isoprene SOA and captured as much as 53% and 33% of organic aerosol in Borneo<sup>12</sup> and Atlanta, Georgia<sup>13</sup> respectively. Modeling studies further support a significant role for later generation isoprene products in forming OC.<sup>14,15</sup>

Traditionally, isoprene SOA has been represented using an Odum 2-product approach<sup>16,17</sup> based on vapor pressure dependent partitioning of semivolatile surrogates. However, both particle water and organics likely serve as partitioning phases,<sup>18</sup> and comparisons of the modern and fossil portions of water-soluble organic carbon (WSOC) and total OC indicate that biogenic OC is preferentially present in the aqueous phase in the eastern United States.<sup>19</sup> Furthermore, known isoprene SOA constituents like the 2-methyltetrols are highly correlated with WSOC in the southeastern U.S. ( $r^2$  of 0.88 in Centreville, Alabama<sup>11</sup>). While both cloud and aerosol water are candidates

Received: May 10, 2013

Revised: July 24, 2013

Accepted: August 26, 2013

**Table 1. New Isoprene SOA Species Considered in the CMAQ Model along with Their Molecular Weight, OM/OC Ratio, Parent Hydrocarbon Identity, Nucleophile That Adds to the Parent, and Rate Constants for H<sup>+</sup> and HSO<sub>4</sub><sup>−</sup> Catalyzed Ring-Opening Reactions<sup>26c</sup>**

species	MW [g mol <sup>−1</sup> ]	OM/OC	parent hydrocarbon	nucleophile added	$k_{\text{H}^+}$ [M <sup>−2</sup> s <sup>−1</sup> ]	$k_{\text{HSO}_4^-}$ [M <sup>−2</sup> s <sup>−1</sup> ]
2-methyltetrol	136	2.27	IEPOX	water	$9.0 \times 10^{-4a}$	$1.3 \times 10^{-5}$
IEPOX-derived OS	216	3.60	IEPOX	sulfate	$2.0 \times 10^{-4b}$	$2.9 \times 10^{-6}$
IEPOX-derived ON	181	3.02	IEPOX	nitrate	$2.0 \times 10^{-4}$	$2.9 \times 10^{-6}$
2-MG	120	2.50	MAE, HMML	water	$9.0 \times 10^{-4}$	$1.3 \times 10^{-5}$
MPAN-derived OS	200	4.17	MAE, HMML	sulfate	$2.0 \times 10^{-4b}$	$2.9 \times 10^{-6}$
MPAN-derived ON	165	3.44	MAE, HMML	nitrate	$2.0 \times 10^{-4}$	$2.9 \times 10^{-6}$
dimers (as tetrol dimer)	248	2.07	IEPOX	2-methyltetrol	$2.0 \times 10^{-4}$	$2.9 \times 10^{-6}$
			IEPOX	IEPOX-derived OS	$2.0 \times 10^{-4}$	$2.9 \times 10^{-6}$
			IEPOX	IEPOX-derived ON	$2.0 \times 10^{-4}$	$2.9 \times 10^{-6}$
			MAE, HMML	2-MG	$2.0 \times 10^{-4}$	$2.9 \times 10^{-6}$
			MAE, HMML	MPAN-derived OS	$2.0 \times 10^{-4}$	$2.9 \times 10^{-6}$
			MAE, HMML	MPAN-derived ON	$2.0 \times 10^{-4}$	$2.9 \times 10^{-6}$

<sup>a</sup>Sensitivity analysis indicates this value is too high, and a value of  $2.0 \times 10^{-4} \text{ M}^{-2} \text{ s}^{-1}$  is more consistent with observations of 2-methyltetrols.

<sup>b</sup>Sensitivity analysis indicates this value might be too low and that additional investigation is needed. <sup>c</sup>OS denotes organosulfate, while ON denotes organonitrate. See Tables S1 and S2 for additional information.

for water-soluble organic partitioning, McNeill et al. indicate that aqueous-phase aerosol processing may result in more OC than in-cloud processing as a result of more concentrated conditions.<sup>20</sup>

Later generation isoprene products with the potential to form SOA have been identified but are not yet widely incorporated into models. Under low-NO<sub>x</sub> conditions in which isoprene peroxy radicals (RO<sub>2</sub>·) react predominantly with hydroperoxal radicals (HO<sub>2</sub>·), isoprene epoxydiols (IEPOX) are formed with a relatively high yield.<sup>21</sup> Under high-NO<sub>x</sub> conditions when the isoprene peroxy radical reacts predominantly with NO, high NO<sub>2</sub>/NO ratios lead to methacryloylperoxynitrate (MPAN) and SOA.<sup>22</sup> MPAN reaction with the hydroxyl radical (·OH) produces methacrylic acid epoxide (MAE)<sup>23</sup> as well as hydroxymethylmethyl-α-lactone (HMML).<sup>24</sup> MAE<sup>23</sup> and HMML<sup>24</sup> have been proposed as the isoprene SOA precursor under high-NO<sub>x</sub> conditions, but the fate of HMML is somewhat uncertain given that similar analogues have short lifetimes.<sup>25</sup> Both epoxides, IEPOX and MAE, can participate in acid-catalyzed ring-opening reactions in the particle phase,<sup>26</sup> and higher isoprene aerosol concentrations have been linked with acidity ([H<sup>+</sup>]) in laboratory experiments<sup>27</sup> and sulfate under ambient conditions.<sup>7</sup>

In this paper, new aerosol-phase aqueous processes are incorporated into CMAQ to predict formation of key aerosol species from IEPOX (low-NO<sub>x</sub>) and MPAN (high-NO<sub>x</sub>). The parent hydrocarbon distribution depends on NO<sub>x</sub>, and the aqueous parametrization is a function of acidity as well as availability of aerosol-phase constituents including water and sulfate. Simulations for summer 2006 over the United States are compared to observations of individual species as well as to isoprene SOA modeled by Odum 2-product partitioning. Parameters with uncertainty are identified, and their effects on model predictions assessed. In addition, the model response to reductions in NO<sub>x</sub> and SO<sub>x</sub> emissions is examined.

## MODEL DESCRIPTION

**Chemical Transport Model.** The Community Multiscale Air Quality (CMAQ) model<sup>28</sup> version 5.0.1 which treats advection, diffusion, gas-phase chemistry, aerosol processes, and deposition is used to simulate June 1 through August 31, 2006 conditions over the contiguous United States at 12 km × 12 km

horizontal resolution with 35 vertical layers. Emissions are based on the 2005 National Emission Inventory (NEI) with year 2006 data for electric generating units and wildfires. Biogenic emissions are predicted inline with BEIS algorithms<sup>6</sup> using meteorology from WRF v3.3 processed by MCIP 4.0.<sup>29</sup> The CMAQ SAPRC07T chemistry<sup>30</sup> is expanded, adding over 150 new reactions and 34 new species, to include formation of IEPOX, MAE, and HMML in the gas phase<sup>23,31</sup> (Figure S1).

**Aerosol-Phase Chemistry.** CMAQ treats accumulation mode aerosol as an internal mixture of organic and inorganic constituents. Secondary inorganic aerosol, including ammonium and nitrate, is predicted using the thermodynamic equilibrium model ISORROPIA II.<sup>32</sup> In this section, we define the base case model parametrization to include isoprene SOA from the Odum 2-product approach<sup>6</sup> in parallel to aerosol from isoprene epoxides with baseline parameters (Figure S1). Deviations from the base case are described in the subsequent section entitled *Sensitivity simulations*.

**Removal of Existing Model Processes.** The standard CMAQ treatment of isoprene SOA is based on an Odum 2-product fit for semivolatile aerosol using low-NO<sub>x</sub> chamber experiments<sup>33</sup> followed by an acid enhancement under conditions of strong acidity and oligomerization of the particle phase to nonvolatile form using a fixed rate constant.<sup>6</sup> In this work, the acid enhancement and oligomerization processes are removed since they are captured in a more mechanistic way by the new parametrization described below. The Odum 2-product semivolatile parametrization is retained as an estimate of semivolatile organic-phase isoprene aerosol production.

**New Processes Added to the Model.** SOA formation from uptake of IEPOX and the sum of MAE and HMML onto aqueous aerosols is added to the model, while aerosol formation in cloud and fog droplets is neglected. For modeling purposes, HMML (57% yield from MPAN + ·OH) is treated like MAE (21% yield from MPAN + ·OH)<sup>23</sup> in terms of heterogeneous uptake, providing an upper bound on the amount of SOA from MPAN.

The conversion of IEPOX and MAE + HMML to aerosol-phase species is accomplished via heterogeneous uptake onto accumulation mode aerosols. Uptake onto the aerosol phase can be parametrized using an uptake coefficient,  $\gamma$ , that can be calculated following<sup>34</sup>

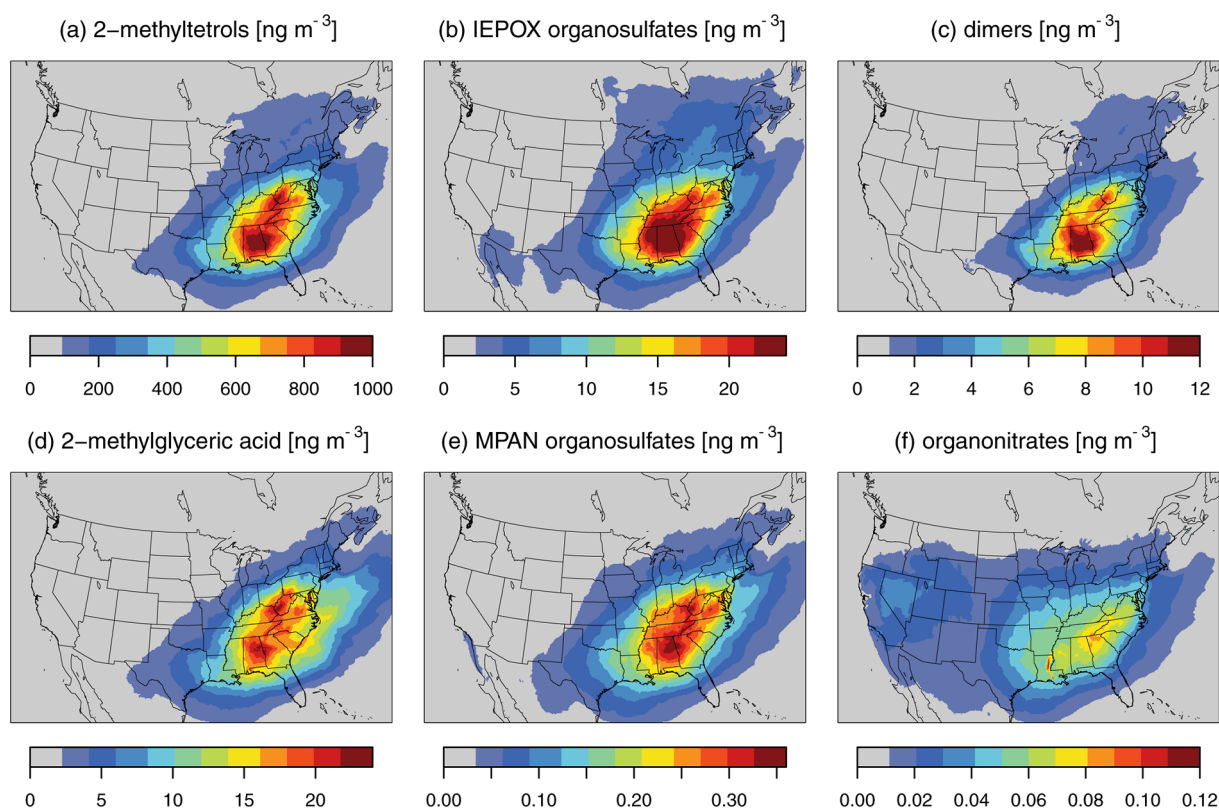


**Figure 1.** Predicted mean concentrations for July–July–August 2006 of (a) 2-methyltetrols, (b) IEPOX-derived organosulfates, (c) isoprene aerosol dimers, (d) 2-MG, (e) MPAN-derived organosulfates, and (f) IEPOX- and MPAN-derived organonitrates for the base simulation.

$$\gamma = \left( \frac{1}{\alpha} + \frac{\nu}{4HRT\sqrt{D_a k_{\text{particle}}}} \frac{1}{f(q)} \right)^{-1} \quad (1)$$

$$f(q) = \coth(q) - \frac{1}{q} \quad (2)$$

$$q = r_p \sqrt{\frac{k_{\text{particle}}}{D_a}} \quad (3)$$

where  $\alpha$  is the mass accommodation coefficient ( $0.02^{20}$ ),  $\nu$  is the mean molecular speed,  $H$  is the Henry's Law coefficient,  $R$  is the gas constant,  $T$  is temperature,  $D_a$  is diffusivity in the aerosol phase ( $1 \times 10^{-9} \text{ m}^2 \text{ s}^{-1}$  <sup>35</sup>),  $k_{\text{particle}}$  is the pseudo-first-order rate constant for reaction of the parent hydrocarbon in the aerosol phase,  $q$  is the diffuso-reactive parameter, and  $r_p$  is the effective particle radius. The Henry's Law coefficients for IEPOX and MAE are estimated to be  $2.7 \times 10^6$  and  $1.2 \times 10^5 \text{ M atm}^{-1}$  using HenryWin 3.2 (bond contribution method<sup>36</sup>).<sup>37</sup> (See the SI for additional details on model parameters and the implementation of uptake coefficients in CMAQ.)

The pseudo-first-order particle-phase rate constant,  $k_{\text{particle}}$ , is calculated assuming protonation of the epoxide oxygen and nucleophilic addition. Eddingsaas et al. determined from information on isotopic effects and NMR analysis that epoxides similar to IEPOX follow an A-2 mechanism in which the rate determining step in the reaction is concerted nucleophilic addition to the ring.<sup>26</sup> We assume the A-2 mechanism applies here; thus the particle-phase rate constant for an epoxide during a given model time step (in which the concentrations of nucleophiles and acids are constant) is

$$k_{\text{particle}} = \sum_{i=1}^N \sum_{j=1}^M k_{i,j} [\text{nuc}_i] [\text{acid}_j] \quad (4)$$

for  $N$  nucleophiles and  $M$  acids. Concentrations are expressed in molarity ( $\text{mol L}^{-1}$ ). Seven new species are added to CMAQ to represent the results of particle phase reactions between nucleophiles and  $\text{H}^+$  (a specific acid) or bisulfate (a general acid)<sup>26</sup> (Table 1). IEPOX (and MAE) form 2-methyltetrols (and 2-MG), organosulfates, and organonitrates as a result of addition of water, sulfate, and nitrate. These species can then serve as nucleophiles that add to an epoxide to form oligomers. Only dimers are currently considered (no higher-order oligomers),<sup>38</sup> and all dimers are lumped together. Currently, there is no precedent for including reactions of epoxides with other organic species in the particle phase, and such additional pathways have not been considered.

Third-order rate constants for the particle-phase reactions ( $k_{i,j}$ ) are based on the work of Eddingsaas et al.<sup>26</sup> and  $\beta$ -IEPOX, the proposed dominant IEPOX isomer mixture,<sup>39</sup> when available (see Tables 1, S1, S2). Due to a lack of kinetic data, the MAE rate constants are assumed to be the same as for IEPOX. However, density functional calculations suggest that the barrier for the acid-catalyzed hydrolysis of MAE is higher than for IEPOX; thus, the rate constant may be considerably smaller.<sup>40</sup>

The concentrations of acids and nucleophiles in eq 4 are accumulation mode concentrations predicted by CMAQ using ISORROPIA II.<sup>32</sup> Concentrations, usually expressed in  $\mu\text{g m}^{-3}$ , are converted to molarity using the entire accumulation mode volume (deviations from ideality are not treated in the kinetic calculations). The concentration of  $\text{H}^+$  is based on the equilibrated Aitken and accumulation modes as calculated by



ISORROPIA II. Since CMAQ transports only total sulfate in the particle, the ISORROPIA II predicted  $\text{H}^+$  along with a charge balance are used to separate  $\text{SO}_4^{2-}$  (nucleophile) and  $\text{HSO}_4^-$  (general acid) for epoxide uptake.

Particle-phase reactions of IEPOX also lead to  $\text{C}_5$ -alkene triols<sup>22</sup> and *cis*- and *trans*-3-methyl-3,4-dihydroxytetrahydrofurans<sup>7</sup> which are not represented in the model. *Cis*- and *trans*-3-methyl-3,4-dihydroxytetrahydrofurans are significantly less abundant than the 2-methyltetrols.<sup>7,41</sup> However,  $\text{C}_5$ -alkene triol concentrations can be significant.<sup>7,41</sup> Since the  $\text{C}_5$ -alkene triols are not explicitly predicted by the model, the predictions of 2-methyltetrols may be overestimated. If the  $\text{C}_5$ -alkene triols also form from IEPOX in the presence of acid and water (hydrolysis), the modeled 2-methyltetrols might encompass both the 2-methyltetrols and  $\text{C}_5$ -alkene triols.<sup>15</sup>

**Sensitivity Simulations.** Sensitivity simulations are performed to examine the effects of changes in the model parameters and emissions. Two sensitivity simulations address uncertainty in the rates of particle-phase reaction and the Henry's Law coefficients (eq 1). The rate constant for a given nucleophile with IEPOX should be related to the nucleophilic strength of that species.<sup>42</sup> Although water is a weaker nucleophile than sulfate, rate constants in Table 1 indicate the opposite trend. Since the sulfate rate constant is based on experiments with nitrate and *cis*-2,3-epoxybutane-1,4-diol (Table S2), future work should better constrain the sulfate rate constant for IEPOX. To test the effect of the third-order  $k_{ij}$  rate constants on predictions of aerosol species, a sensitivity simulation is performed in which all the  $k_{ij}$  are set equal to the nitrate value (*sensitivity*  $k_{ij}$ ). This sensitivity simulation affects the relative tetrol to organosulfate split and thus the particle-phase speciation.

Chan et al.<sup>43</sup> estimated the Henry's Law coefficient of IEPOX to be  $1.9 \times 10^7 \text{ M atm}^{-1}$ , roughly a factor of 7 higher than our baseline value. The second sensitivity simulation (*sensitivity*  $H\text{-law}, k_{ij}$ ) uses the nitrate-based rate constant from the first sensitivity simulation in addition to higher Henry's Law coefficients: the Chan et al. value for IEPOX<sup>43</sup> ( $1.9 \times 10^7 \text{ M atm}^{-1}$ ) and  $1.2 \times 10^6 \text{ M atm}^{-1}$  (10 $\times$  higher than the baseline) for MAE. To a certain extent, this sensitivity simulation captures uncertainty in the Henry's Law coefficient as well as the overall particle-phase rate of reaction. It is expected to increase the overall magnitude of organic aerosol production while maintaining a speciation similar to *sensitivity*  $k_{ij}$ . Changes to the estimated Henry's Law coefficient also affect wet scavenging but not dry deposition.

Two additional simulations examine the impact of reductions in emissions on isoprene SOA. Both emission control scenarios, a 25% reduction in anthropogenic and wildfire  $\text{NO}_x$  and a 25% reduction in all  $\text{SO}_x$  ( $\text{SO}_2 + \text{SO}_4^{2-}$ ), are performed for July 2006 with the base model parametrization of heterogeneous uptake. All simulations contain traditional Odum 2-product semivolatile SOA in parallel to the new epoxide SOA (Figure S1).

## RESULTS AND DISCUSSION

**Model Predictions. Base Simulation.** The new aerosol species are highest in concentration (Figure 1) where high rates of particle-phase reaction (Figure S3) coincide with significant isoprene emissions (Figure S2) allowing uptake of epoxides to the aerosol phase to compete with gas-phase  $\cdot\text{OH}$  reaction. The rate of particle-phase reaction is primarily governed by the rate of  $\text{H}^+$  catalyzed ring-opening accompanied by addition of water

producing 2-methyltetrols and 2-MG. The pseudo-first-order particle-phase rate constants are highest (0.02 to  $0.03 \text{ s}^{-1}$ ) where  $\text{H}^+$  is also highest such as downwind of the Ohio River Valley during the modeled period (Figure S3(a)). This leads to significant isoprene aerosol over West Virginia, but the highest isoprene aerosol concentrations tend to be over Alabama, where the concentration of IEPOX is higher.

Of the IEPOX-derived species, the hydrolysis products (2-methyltetrols) are predicted to dominate as a result of the relative abundance of aerosol water compared to other available nucleophiles. The organonitrates from IEPOX and MPAN are predicted to be the least abundant species due to low nitrate aerosol concentrations during the summer. A contribution to 2-methyltetrols and organosulfates from further reaction of organonitrates in the atmosphere<sup>44</sup> is not considered here because of the low concentrations of aerosol organonitrates in summer. The isoprene aerosol dimers (composed mostly of tetrol–tetrol dimers) are significantly less abundant than the monomers, while the IEPOX organosulfates and 2-MG are comparable in magnitude.

Aerosol from IEPOX generally exceeds the aerosol from MAE as a result of availability of gas-phase precursors (Figure S2) as well as the efficiency of uptake. Since IEPOX and MAE are treated the same in terms of particle-phase reaction rates, the difference in the uptake coefficients for MAE and IEPOX is entirely attributable to the difference in their Henry's Law coefficients. The IEPOX uptake coefficient predicted here is similar in magnitude to that of glyoxal ( $2.9 \times 10^{-3}$ )<sup>45</sup> in locations of very high acidity but lower elsewhere and generally below  $10^{-3}$  across the Southeast. The factor of 20 lower Henry's Law coefficient for MAE compared to IEPOX leads to a similarly lower value of the uptake coefficient ( $1.4 \times 10^{-4}$  or less) (Figure S3).

**Vertical Profiles.** Models underestimate organic aerosol throughout the troposphere and particularly for the lower 2 km of the atmosphere in many pollution-influenced locations.<sup>46,47</sup> Cloud-Aerosol Lidar with Orthogonal Polarization (CALIOP) instrument data further indicate that aerosol extinction is dominated by aerosols below 700 hPa (3 km) in the southeastern US.<sup>48</sup> Model bias aloft has been shown to be a function of relative humidity, indicating a role for aqueous aerosol processing.<sup>47</sup> The heterogeneous pathways implemented here lead to aerosol that is mostly confined to the lower 2 km of the atmosphere (Figure S5), similar to the aerosol of Couvidat et al.,<sup>15</sup> and different from the aqueous aerosol of Fu et al.<sup>49</sup> which peaked between 2 and 6 km. In addition, the new aerosol exceeds that from traditional semivolatile partitioning of isoprene products by more than 50% from 0.5 to 2.7 km, making it a candidate to close the measurement-model gap in the vertical distribution of organic aerosol. Note that the predicted vertical profile of MPAN-derived aerosol in this work indicates little support for higher 2-MG relative to IEPOX-derived aerosol despite MPAN reaction with  $\cdot\text{OH}$  increasing relative to thermal loss with altitude (Figure S5).

**Uncertainty Analysis.** Across the eastern US, hydrolysis product (2-methyltetrol and 2-MG) and IEPOX-derived organosulfate concentrations vary significantly from the base case simulation due to changes in the third-order particle-phase reaction rate constants and Henry's Law coefficients (Figure 2). Decreasing the  $k_{ij}$  for nucleophilic addition of water (*sensitivity*  $k_{ij}$ ) decreases the hydrolysis products but leads to increases in the organosulfates as a result of less competition with water

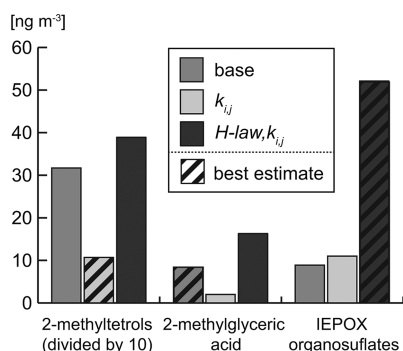


**Figure 2.** Effect of sensitivity simulations on three major isoprene-derived aerosol-phase constituents for June-July-August 2006. Sensitivity  $k_{ij}$  reduces the rate constant for nucleophilic addition of water to the value used for nitrate ( $2 \times 10^{-4} \text{ M atm}^{-1}$ , Table 1). Sensitivity  $H\text{-law}, k_{ij}$  uses the same particle-phase rate constants as sensitivity  $k_{ij}$  but increases the Henry's law coefficients by a factor of 7 and 10 for IEPOX and MAE, respectively. Concentrations are averaged over a 2,412 km by 2,052 km portion of the eastern United States. Predictions with the best agreement with observations are indicated with diagonal lines.

addition. Increasing the Henry's Law coefficients (*sensitivity  $H\text{-law}, k_{ij}$* ) scales up the concentrations of aerosol species while roughly maintaining the relative ratios in *sensitivity  $k_{ij}$* . Note that organosulfates increase significantly in *sensitivity  $H\text{-law}, k_{ij}$*  which has both the lower rate constant for nucleophilic addition of water and higher Henry's Law coefficient.

**Comparison to Observations.** Many of the new species, including 2-methyltetrols, 2-MG, and organosulfates, added to the model have been observed in the atmosphere, which allows for model evaluation. However, the spatial and temporal coverage of measurements is limited, which makes a quantitative evaluation across a large domain challenging. For individual species evaluation, we present the sensitivity simulations having the best agreement with observations (indicated in Figure 2 with diagonal lines).

**Hydrolysis Products.** Daily integrated samples of 2-methylthreitol + 2-methylerythritol (both 2-methyltetrols) and 2-MG collected every sixth day during 2006 in Research Triangle Park (RTP), North Carolina<sup>50</sup> are paired in time and space with the model results. The base simulation for IEPOX tends to significantly overestimate 2-methyltetrols implying that tetrols may form less efficiently than our a priori parameters suggest or that IEPOX is overestimated. The lower rate constant for hydrolysis reactions ( $4.5\times$  lower, *sensitivity  $k_{ij}$* ) leads to the best agreement with 2-methyltetrol observations (depicted in Figure 3) but still overestimates 2-methyltetrol concentrations by  $97 \text{ ng m}^{-3}$  (107%) on average at RTP. Overestimates may arise from the absence of a competitive loss process of IEPOX to  $C_5$ -alkene triols. The base simulation (Figure 3, 2-MG), is able to capture 2-MG concentrations relatively well with only a  $-0.8 \text{ ng m}^{-3}$  mean bias ( $-5\%$  normalized mean bias).

Model predictions of semivolatile Odum 2-product isoprene SOA can be converted to estimates of 2-methyltetrols + 2-MG using composition information from laboratory experiments, providing a rough evaluation of traditional semivolatile SOA for comparison to the new pathways. Laboratory experiments report that 2-methyltetrols and 2-MG account for 6.3% of isoprene-derived SOA.<sup>9</sup> Included in Figure 3 is the sum of hydrolysis products (2-methyltetrols and 2-MG) calculated

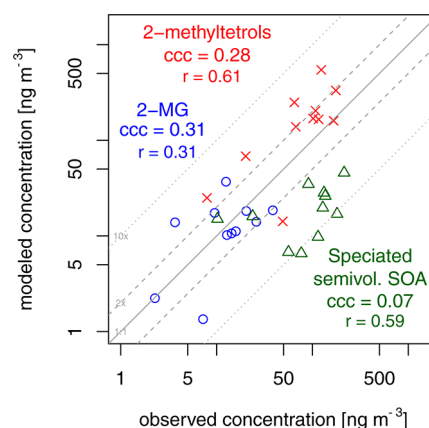


**Figure 3.** Observed<sup>50</sup> and predicted concentrations of 2-methyltetrols (red x) and 2-MG (blue circle) in Research Triangle Park, North Carolina during 2006. Also shown is the calculated sum 2-methyltetrols and 2-MG (green triangle) based on speciating semivolatile isoprene SOA with a laboratory based factor. The concordance correlation coefficient (ccc) and Pearson  $r$  are shown for each set of model-observation pairs. Model results are only shown for the sensitivity simulations indicated by diagonal lines in Figure 2

using the laboratory speciation factor of 6.3% and Odum 2-product isoprene SOA. The concordance correlation coefficient (ccc),<sup>51,52</sup> a measure of both precision and accuracy, indicates that the new heterogeneous pathways (ccc = 0.31 for 2-MG, ccc = 0.28 for 2-methyltetrols) produce concentrations of isoprene aerosol constituents that are more consistent with observations than the traditional semivolatile absorptive partitioning pathway (ccc = 0.07 for speciated Odum 2-product semivolatile isoprene SOA). The ccc for 2-methyltetrols from IEPOX could be further improved by additional decreases in the  $k_{\text{water}, H^+}$  rate constant below the *sensitivity  $k_{ij}$*  value. Using the rate constant for  $\delta$ -IEPOX hydrolysis of  $1.4 \times 10^{-4} \text{ M}^{-2} \text{ s}^{-1}$ , for example,<sup>53</sup> leads to a ccc of 0.39 and a mean bias of  $49 \text{ ng m}^{-3}$  (54% normalized mean bias).

Measurements of isoprene aerosol species from additional campaigns and time periods other than 2006 are compared to modeled June-July-August 2006 concentrations to understand whether the new model captures spatial patterns (Figure 4 and abstract figure). Since the observations are not paired in time and campaigns may have targeted certain pollution events, the comparison should be viewed as illustrative, but the difference in concentrations between broad geographic regions such as California and the Southeast is expected to be relatively robust. Only model predictions from the simulations with best agreement (as determined by the RTP 2006 data) are shown. Most of the 2-methyltetrol comparisons fall within the factor of 2 range and indicate the model is capturing differences in locations such as California and the midwestern United States. Methylglyceric acid is not captured as well, and modeled concentrations are more than a factor of 10 lower than observations for Bakersfield, California and Riverside, California (from 2010 and 2005, respectively). Gas-phase concentrations of MAE are predicted to exceed  $100 \text{ ng m}^{-3}$  in the model for Southern California<sup>23</sup> which would provide more than enough precursor to achieve the 2-MG concentrations observed, but minimal uptake to the aerosol phase occurs.

**Organosulfates.** Due to the limited duration of sampling campaigns, only a qualitative evaluation of the organosulfate concentrations predicted here is possible. The IEPOX organo-

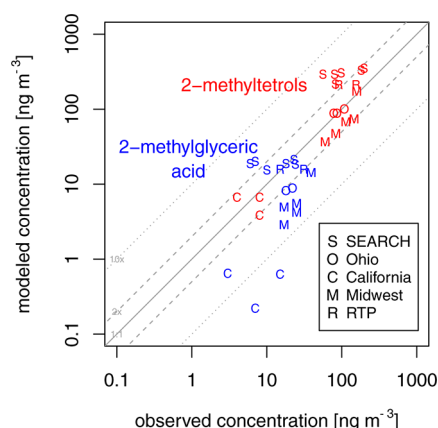


**Figure 4.** Observed and modeled concentrations of isoprene aerosol species across the United States. Observations include measurements from SEARCH sites in 2005<sup>57</sup> and 2008<sup>43</sup> (S), the Cleveland Multiple Air Pollutant Study in Ohio during 2009 (O),<sup>10,56</sup> Pasadena and Bakersfield (California Research at the Nexus of Air Quality and Climate Change, CalNex, 2010), and Riverside (Study of Organic Aerosols in Riverside, SOAR, 2005) in California (C),<sup>10</sup> the Midwest Urban Organics Study in 2004 (M),<sup>8</sup> and Research Triangle Park in North Carolina during 2003<sup>58</sup> and 2006<sup>50</sup> (R). Observations are limited to May through September and compared to a model June–July–August 2006 average for each location. Model results are only shown for the sensitivity simulations indicated by diagonal lines in Figure 2. The information is also presented graphically in the abstract.

sulfate (molecular weight = 216 g mol<sup>−1</sup>) has been detected at levels up to 515 ng m<sup>−3</sup> (approximately 100 ng m<sup>−3</sup> on average<sup>7</sup>) at the surface and 84 ng m<sup>−3</sup> on average aloft in the troposphere.<sup>54</sup> The MPAN organosulfate (2-MG sulfate ester) is less abundant in both the model results and observed concentrations for Yorkville, Georgia, where concentrations average 10 ng m<sup>−3</sup>.<sup>7</sup> Our model results suggest efficient formation of the IEPOX organosulfate at concentrations of 25 to 150 ng m<sup>−3</sup> as a seasonal average in the southeastern United States with perhaps the best agreement with measurements from Yorkville, Georgia, in 2010<sup>7</sup> for the most aggressive uptake (*sensitivity H-law,  $k_{ij}$* ). The MPAN organosulfate concentrations from the base simulation are predicted to be less than 1 ng m<sup>−3</sup> and could be significantly underestimated.

**Total OC.** Addition of aerosol from IEPOX and MPAN improves model performance of total OC in terms of magnitude and diurnal variation. Without the heterogeneous uptake pathways for IEPOX and MAE + HMML, CMAQ underestimates total OC by 1.15  $\mu\text{gC m}^{-3}$  compared to the Chemical Speciation Network (CSN) and 0.29  $\mu\text{gC m}^{-3}$  compared to the IMPROVE network during June–July–August 2006. The most aggressive uptake scenario examined (*sensitivity H-law,  $k_{ij}$* ) is able to reduce that underestimate by 17% for CSN and 34% for IMPROVE. Observations from the Southeastern Aerosol Research and Characterization (SEARCH) study of OC indicate a relatively flat diurnal profile, while earlier versions of CMAQ<sup>6</sup> tend to have a pronounced nighttime high driven by primary organic aerosols and monoterpene + nitrate radical aerosol with additional influences from sesquiterpene SOA. The new isoprene SOA has a flatter diurnal profile with a slight daytime peak (Figures S6 and S7), which helps move the diurnal profile toward OC observations. Further supporting the heterogeneous uptake pathway as reasonable are the observed diurnal patterns of WSOC in Yorkville and Atlanta<sup>55</sup> and IEPOX-OA in Atlanta, Georgia,<sup>13</sup> which tend to be relatively

flat or peak during the day. If the epoxide aerosol mechanism implemented in CMAQ is representative of IEPOX-OA<sup>13</sup> and can be scaled up to be consistent with the 33% contribution to total OA observed by Budisulistiorini et al.,<sup>13</sup> it would effectively reduce the day/night imbalance in CMAQ in the Southeast.

**Relative Roles of IEPOX and MPAN Aerosol.** Observations<sup>7–10,43,50,56–58</sup> indicate that IEPOX-derived 2-methyltetrols generally dominate over MPAN-derived 2-MG, particularly during the summer. Exceptions to this trend include measurements taken downwind of Siberian biomass burning plumes,<sup>59</sup> wintertime aerosol in the midwestern United States,<sup>8</sup> and samples from Riverside and Bakersfield, California.<sup>10</sup> In all exceptional cases, high-NO<sub>x</sub> conditions as a result of proximity to NO<sub>x</sub> emissions or higher NO to HO<sub>2</sub>· ratios (as expected in winter,<sup>60,61</sup>) likely lead to enhanced 2-MG formation as a result of enhanced RO<sub>2</sub>· + NO reactions. The model is generally consistent with data supporting the dominance of 2-methyltetrols at the surface and aloft in the southeast United States.

The dominance of 2-methyltetrols over 2-MG can be explained by the pathways leading to their production and the relative amounts of their gas-phase precursors. Formation of IEPOX begins with isoprene reacting with ·OH followed by HO<sub>2</sub>· to form hydroxyhydroperoxides (ISOPOOH). Further reaction of ISOPOOH with ·OH produces IEPOX in mass-based yields up to 61% under typical summertime conditions in the southeastern United States.<sup>21,31</sup> Formation of MAE requires isoprene peroxyradicals to initially react with NO, decomposing to create methacrolein, followed by three more reactions forming MPAN and then MAE.<sup>23</sup> Along the way, carbon is lost via competitive pathways that produce methylvinyl ketone and other species, thus, less than 5% of the initial isoprene forms MAE or HMML under typical southeastern U.S. conditions. Only when the rate of RO<sub>2</sub>· + NO exceeds RO<sub>2</sub>· + HO<sub>2</sub>· by a factor of 9 are the precursors to 2-MG expected to exceed IEPOX. These conditions could occur in NO<sub>x</sub> source areas (e.g., urban areas) or during the winter. The higher Henry's Law coefficient for IEPOX compared to MAE also leads to higher 2-methyltetrol concentrations relative to 2-MG. If the acid-catalyzed ring-opening of MAE is slower than estimated here<sup>40</sup> as in *sensitivity  $k_{ij}$* , the model would likely underestimate 2-MG even more.

**Implications of Emission Reductions for Isoprene SOA.** *Effect of NO<sub>x</sub>.* Enhancements in biogenic SOA have been attributed to NO<sub>x</sub> in the ambient atmosphere,<sup>62</sup> but models examining the same effect<sup>63,64</sup> have not considered the dependence of SOA yield on peroxy radical fate as demonstrated here. For a 25% reduction in NO<sub>x</sub>, semivolatile isoprene SOA is predicted to decrease (Figure 5), consistent with previous studies.<sup>6</sup> In contrast, IEPOX-derived aerosol increases as the isoprene RO<sub>2</sub>· fate is shifted away from the NO pathway and toward reaction with HO<sub>2</sub>·. This shift also leads to decreased MPAN-derived aerosol, but the change in the absolute magnitude of that aerosol is quite small in comparison to the IEPOX path (Figure S8). Since semivolatile aerosol production decreases while IEPOX-derived aerosol generally increases, the relative role of these production pathways would determine the response of total isoprene aerosol (Figure S10(a)).

Inclusion of additional model processes could alter the response of isoprene SOA to reductions in NO<sub>x</sub>. Aerosol from isoprene + NO<sub>3</sub>· could contribute about one-quarter of



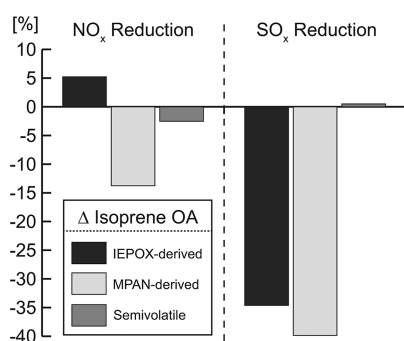


**Figure 5.** Predicted percent change in IEPOX-derived, MPAN-derived, and semivolatile (Odum 2-product) isoprene SOA over the eastern United States for a 25% reduction in anthropogenic and wildfire-derived NO<sub>x</sub> and a 25% reduction in SO<sub>x</sub> relative to a base simulation for July 2006. The effect on isoprene dimers (a minor species) is not shown.

isoprene aerosol<sup>65</sup> and one-third of all aerosol generated at night.<sup>66</sup> Reductions in NO<sub>x</sub> should lead to decreases in the NO<sub>3</sub> pathway thus at least partially offsetting the increase in IEPOX aerosol. However, this pathway is not yet represented in the model. The results presented here also do not capture formation of aerosol from glyoxal and methylglyoxal which should decrease under lower-NO<sub>x</sub> conditions.<sup>20</sup>

**Effect of SO<sub>x</sub>.** Most sulfate and almost all SO<sub>2</sub> emitted in the United States is of anthropogenic origin.<sup>64,67</sup> All of the epoxide aerosol, including the dominant isoprene aerosol species, 2-methyltetrols, depends on acidity and is thus subject to regulation by emissions of SO<sub>x</sub>. A 25% reduction in SO<sub>x</sub> is predicted to lead to a significant decrease in isoprene aerosol (Figure 5). The effect on semivolatile Odum 2-product isoprene aerosol is minor. However, both IEPOX- and MPAN-derived aerosol are significantly reduced as less acidity leads to slower rates of particle-phase reaction and less efficient uptake. Conversion of epoxides to the aerosol phase is further reduced by decreases in particle surface area. Changes in IEPOX-derived aerosol dominate the overall change in isoprene aerosol from all three pathways (Figure S9) resulting in predicted decreases up to 400–450 ng m<sup>-3</sup> over the eastern United States. The decrease in isoprene SOA due to a reduction in SO<sub>x</sub> is roughly a factor of 10 higher than the response due to a reduction in NO<sub>x</sub> (Figure S10), making SO<sub>x</sub> the likely anthropogenic control on epoxide-derived SOA in the eastern United States.

**Future Directions.** While this new model framework makes considerable progress in addressing formation of specific isoprene aerosol constituents with significant ambient concentrations, a complete description of isoprene aerosol, including glyoxal and methylglyoxal, and an expansion of processes examined here to the cloud phase is still needed to accurately capture how changes in anthropogenic emissions affect biogenic SOA. The sensitivity simulations employed here indicate a need to constrain the relative rates of particle-phase reactions leading to tetrols, organosulfates, and oligomers since organosulfates seem to form much more readily in the ambient than our a priori parametrization predicts (possibly due to an underestimated  $k_{\text{SO}_4^{2-}, \text{H}^+}$ ); and, although we have focused on the explicit production of seven isoprene aerosol species, isoprene can lead to additional aerosol in the atmosphere. Experiments connecting total IEPOX and MAE aerosol mass to the individual species would allow for improved attribution of

ambient OC to isoprene. Ambient observations of classes or groups of compounds such as XRF sulfur-IC sulfate estimates of organosulfates<sup>68</sup> and AMS PMF factors<sup>12,13</sup> also need to be connected to these and other explicit estimates of specific isoprene SOA constituents.

## ■ ASSOCIATED CONTENT

### Supporting Information

Additional equations, figures, and documentation are available. This material is available free of charge via the Internet at <http://pubs.acs.org>.

## ■ AUTHOR INFORMATION

### Corresponding Author

\*E-mail: [pye.havala@epa.gov](mailto:pye.havala@epa.gov).

### Present Address

‡Shanghai Meteorological Service, Shanghai, China.

### Notes

The authors declare no competing financial interest.

## ■ ACKNOWLEDGMENTS

The authors thank Prakash Bhawe, Golam Sarwar, Wyatt Appel, and Sergey Napelenok for useful discussion as well as SEARCH, CSN, and IMPROVE networks for data. The United States Environmental Protection Agency (EPA) through its Office of Research and Development funded and managed the research described here. This paper has been subjected to the Agency's administrative review and approved for publication. S.L.C. was supported by an appointment to the Research Participation Program at the Office of Research and Development, US EPA, administered by ORISE. Y.-H.L. and J.D.S. were supported in part by the Electric Power Research Institute. Y.-H.L. acknowledges a Dissertation Completion Fellowship from the UNC Graduate School.

## ■ REFERENCES

- (1) Zhang, Q. et al. Ubiquity and dominance of oxygenated species in organic aerosols in anthropogenically-influenced Northern Hemisphere midlatitudes. *Geophys. Res. Lett.* **2007**, *34*.
- (2) Goldstein, A. H.; Koven, C. D.; Heald, C. L.; Fung, I. Y. Biogenic carbon and anthropogenic pollutants combine to form a cooling haze over the southeastern United States. *Proc. Natl. Acad. Sci. U.S.A.* **2009**, *106*, 8835–8840.
- (3) Lewis, C. W.; Klouda, G. A.; Ellenson, W. D. Radiocarbon measurement of the biogenic contribution to summertime PM<sub>2.5</sub> ambient aerosol in Nashville, TN. *Atmos. Environ.* **2004**, *38*, 6053–6061.
- (4) Glasius, M.; la Cour, A.; Lohse, C. Fossil and nonfossil carbon in fine particulate matter: A study of five European cities. *J. Geophys. Res.: Atmos.* **2011**, *116*.
- (5) Guenther, A.; Karl, T.; Harley, P.; Wiedinmyer, C.; Palmer, P. I.; Geron, C. Estimates of global terrestrial isoprene emissions using MEGAN (Model of Emissions of Gases and Aerosols from Nature). *Atmos. Chem. Phys.* **2006**, *6*, 3181–3210.
- (6) Carlton, A. G.; Bhawe, P. V.; Napelenok, S. L.; Edney, E. D.; Sarwar, G.; Pinder, R. W.; Pouliot, G. A.; Houyoux, M. Model representation of secondary organic aerosol in CMAQv4.7. *Environ. Sci. Technol.* **2010**, *44*, 8553–8560.
- (7) Lin, Y.-H.; Knipping, E. M.; Edgerton, E. S.; Shaw, S. L.; Surratt, J. D. Investigating the influences of SO<sub>2</sub> and NH<sub>3</sub> levels on isoprene-derived secondary organic aerosol formation using conditional sampling approaches. *Atmos. Chem. Phys.* **2013**, *13*, 3095–3134.
- (8) Lewandowski, M.; Jaoui, M.; Offenberg, J. H.; Kleindienst, T. E.; Edney, E. O.; Sheesley, R. J.; Schauer, J. J. Primary and secondary



contributions to ambient PM in the midwestern United States. *Environ. Sci. Technol.* **2008**, *42*, 3303–3309.

(9) Kleindienst, T. E.; Jaoui, M.; Lewandowski, M.; Offenberg, J. H.; Lewis, C. W.; Bhawe, P. V.; Edney, E. O. Estimates of the contributions of biogenic and anthropogenic hydrocarbons to secondary organic aerosol at a southeastern US location. *Atmos. Environ.* **2007**, *41*, 8288–8300.

(10) Lewandowski, M.; Piletic, I. R.; Kleindienst, T. E.; Offenberg, J. H.; Beaver, M. R.; Jaoui, M.; Docherty, K. S.; Edney, E. O. Secondary organic aerosol characterization at field sites across the United States during the spring-summer period. *Int. J. Environ. Anal. Chem.* **2013**, DOI: 10.1080/03067319.2013.803545.

(11) Ding, X.; Zheng, M.; Yu, L.; Zhang, X.; Weber, R. J.; Yan, B.; Russell, A. G.; Edgerton, E. S.; Wang, X. Spatial and seasonal trends in biogenic secondary organic aerosol tracers and water-soluble organic carbon in the southeastern United States. *Environ. Sci. Technol.* **2008**, *42*, 5171–5176.

(12) Robinson, N. H.; et al. Evidence for a significant proportion of secondary organic aerosol from isoprene above a maritime tropical forest. *Atmos. Chem. Phys.* **2011**, *11*, 1039–1050.

(13) Budisulistiorini, S. H.; Canagaratna, M. R.; Croteau, P. L.; Marth, W. J.; Baumann, K.; Edgerton, E. S.; Shaw, S. L.; Knipping, E.; Worsnop, D. R.; Jayne, J. T.; Gold, A.; Surratt, J. D. Real-time continuous characterization of secondary organic aerosol derived from isoprene epoxydiols (IEPOX) in downtown Atlanta, Georgia, using the Aerodyne Aerosol Chemical Speciation Monitor (ACSM). *Environ. Sci. Technol.* **2013**, *47*, 5686–5694.

(14) Lin, G.; Penner, J. E.; Sillman, S.; Taraborrelli, D.; Lelieveld, J. Global modeling of SOA formation from dicarbonyls, epoxides, organic nitrates and peroxides. *Atmos. Chem. Phys.* **2012**, *12*, 4743–4774.

(15) Couvidat, F.; Sartelet, K.; Seigneur, C. Investigating the impact of aqueous-phase chemistry and wet deposition on organic aerosol formation using a molecular surrogate modeling approach. *Environ. Sci. Technol.* **2012**, *47*, 914–922.

(16) Henze, D. K.; Seinfeld, J. H. Global secondary organic aerosol from isoprene oxidation. *Geophys. Res. Lett.* **2006**, *33*.

(17) Carlton, A. G.; Wiedinmyer, C.; Kroll, J. H. A review of secondary organic aerosol (SOA) formation from isoprene. *Atmos. Chem. Phys.* **2009**, *9*, 4987–5005.

(18) Zhang, X. L.; Liu, J. M.; Parker, E. T.; Hayes, P. L.; Jimenez, J. L.; de Gouw, J. A.; Flynn, J. H.; Grossberg, N.; Lefer, B. L.; Weber, R. J. On the gas-particle partitioning of soluble organic aerosol in two urban atmospheres with contrasting emissions: 1. Bulk water-soluble organic carbon. *J. Geophys. Res.: Atmos.* **2012**, *117*.

(19) Wozniak, A. S.; Bauer, J. E.; Dickhut, R. M. Characteristics of water-soluble organic carbon associated with aerosol particles in the eastern United States. *Atmos. Environ.* **2012**, *46*, 181–188.

(20) McNeill, V. F.; Woo, J. L.; Kim, D. D.; Schwi, A. N.; Wannell, N. J.; Sumner, A. J.; Barakat, J. M. Aqueous-phase secondary organic aerosol and organosulfate formation in atmospheric aerosols: A modeling study. *Environ. Sci. Technol.* **2012**, *46*, 8075–8081.

(21) Paulot, F.; Crounse, J. D.; Kjaergaard, H. G.; Kurten, A.; St Clair, J. M.; Seinfeld, J. H.; Wennberg, P. O. Unexpected epoxide formation in the gas-phase photooxidation of isoprene. *Science* **2009**, *325*, 730–733.

(22) Surratt, J. D.; Chan, A. W. H.; Eddingsaas, N. C.; Chan, M.; Loza, C. L.; Kwan, A. J.; Hersey, S. P.; Flagan, R. C.; Wennberg, P. O.; Seinfeld, J. H. Reactive intermediates revealed in secondary organic aerosol formation from isoprene. *Proc. Natl. Acad. Sci. U.S.A.* **2010**, *107*, 6640–6645.

(23) Lin, Y.-H.; et al. Epoxide as a precursor to secondary organic aerosol formation from isoprene photooxidation in the presence of nitrogen oxides. *Proc. Natl. Acad. Sci. U.S.A.* **2013**, *110*, 6718–6723.

(24) Kjaergaard, H. G.; Knap, H. C.; Orsso, K. B.; Jorgensen, S.; Crounse, J. D.; Paulot, F.; Wennberg, P. O. Atmospheric fate of methacrolein. 2. Formation of lactone and implications for organic aerosol production. *J. Phys. Chem. A* **2012**, *116*, 5763–5768.

(25) Chen, S.-Y.; Lee, Y.-P. Transient infrared absorption of  $t$ -CH<sub>3</sub>C(O)OO,  $c$ -CH<sub>3</sub>C(O)OO, and  $\alpha$ -lactone recorded in gaseous reactions of CH<sub>3</sub>CO and O-2. *J. Chem. Phys.* **2010**, *132*.

(26) Eddingsaas, N. C.; VanderVelde, D. G.; Wennberg, P. O. Kinetics and products of the acid-catalyzed ring-opening of atmospherically relevant butyl epoxy alcohols. *J. Phys. Chem. A* **2010**, *114*, 8106–8113.

(27) Surratt, J. D.; Lewandowski, M.; Offenberg, J. H.; Jaoui, M.; Kleindienst, T. E.; Edney, E. O.; Seinfeld, J. H. Effect of acidity on secondary organic aerosol formation from isoprene. *Environ. Sci. Technol.* **2007**, *41*, 5363–5369.

(28) Foley, K. M.; Roselle, S. J.; Appel, K. W.; Bhawe, P. V.; Pleim, J. E.; Otte, T. L.; Mathur, R.; Sarwar, G.; Young, J. O.; Gilliam, R. C.; Nolte, C. G.; Kelly, J. T.; Gilliland, A. B.; Bash, J. O. Incremental testing of the Community Multiscale Air Quality (CMAQ) modeling system version 4.7. *Geosci. Model Dev.* **2010**, *3*, 205–226.

(29) Otte, T. L.; Pleim, J. E. The Meteorology-Chemistry Interface Processor (MCIP) for the CMAQ modeling system: Updates through MCIPv3.4.1. *Geosci. Model Dev.* **2010**, *3*, 243–256.

(30) Hutzell, W. T.; Luecken, D. J.; Appel, K. W.; Carter, W. P. L. Interpreting predictions from the SAPRC07 mechanism based on regional and continental simulations. *Atmos. Environ.* **2012**, *46*, 417–429.

(31) Xie, Y.; Paulot, F.; Carter, W. P. L.; Nolte, C. G.; Luecken, D. J.; Hutzell, W. T.; Wennberg, P. O.; Cohen, R. C.; Pinder, R. W. Understanding the impact of recent advances in isoprene photo-oxidation on simulations of regional air quality. *Atmos. Chem. Phys.* **2013**, *13*, 8439–8455.

(32) Fountoukis, C.; Nenes, A. ISORROPIA II: A computationally efficient thermodynamic equilibrium model for  $K^+$ - $Ca^{2+}$ - $Mg^{2+}$ - $NH_4^+$ - $Na^+$ - $SO_4^{2-}$ - $NO_3^-$ - $Cl^-$ - $H_2O$  aerosols. *Atmos. Chem. Phys.* **2007**, *7*, 4639–4659.

(33) Kroll, J. H.; Ng, N. L.; Murphy, S. M.; Flagan, R. C.; Seinfeld, J. H. Secondary organic aerosol formation from isoprene photooxidation. *Environ. Sci. Technol.* **2006**, *40*, 1869–1877.

(34) Hanson, D. R.; Ravishankara, A. R.; Solomon, S. Heterogeneous reactions in sulfuric acid aerosols: A framework for model calculations. *J. Geophys. Res.* **1994**, *99*, 3615–3629.

(35) Gharagheizi, F.; Eslamimanesh, A.; Mohammadi, A. H.; Richon, D. Representation and prediction of molecular diffusivity of non-electrolyte organic compounds in water at infinite dilution using the artificial neural network-group contribution method. *J. Chem. Eng. Data* **2011**, *56*, 1741–1750.

(36) Meylan, W. M.; Howard, P. H. Bond contribution method for estimating Henry's law constants. *Environ. Toxicol. Chem.* **1991**, *10*, 1283–1293.

(37) USEPA, Estimate Programs Interface Suite for Microsoft Windows, v4.11. 2012.

(38) Birdsall, A. W.; Zentener, C. A.; Elrod, M. J. Study of the kinetics and equilibria of the oligomerization reactions of 2-methylglyceric acid. *Atmos. Chem. Phys.* **2013**, *13*, 3097–3109.

(39) Paulot, F.; Crounse, J. D.; Kjaergaard, H. G.; Kroll, J. H.; Seinfeld, J. H.; Wennberg, P. O. Isoprene photooxidation: new insights into the production of acids and organic nitrates. *Atmos. Chem. Phys.* **2009**, *9*, 1479–1501.

(40) Piletic, I. R.; Edney, E. D.; Bartolotti, L. J. A computational study of acid catalyzed aerosol reactions of atmospherically relevant epoxides. *Phys. Chem. Chem. Phys.* **2013** (DOI: 10.1039/C3CP52851K).

(41) Lin, Y.-H.; Zhang, Z.; Docherty, K. S.; Zhang, H.; Budisulistiorini, S. H.; Rubitschun, C. L.; Shaw, S. L.; Knipping, E. M.; Edgerton, E. S.; Kleindienst, T. E.; Gold, A.; Surratt, J. D. Isoprene epoxydiols as precursors to secondary organic aerosol formation: Acid-catalyzed reactive uptake studies with authentic compounds. *Environ. Sci. Technol.* **2012**, *46*, 250–258.

(42) Minerath, E. C.; Schultz, M. P.; Elrod, M. J. Kinetics of the reactions of isoprene-derived epoxides in model tropospheric aerosol solutions. *Environ. Sci. Technol.* **2009**, *43*, 8133–8139.

- (43) Chan, M. N.; Surratt, J. D.; Claeys, M.; Edgerton, E. S.; Tanner, R. L.; Shaw, S. L.; Zheng, M.; Knipping, E. M.; Eddingsaas, N. C.; Wennberg, P. O.; Seinfeld, J. H. Characterization and quantification of isoprene-derived epoxydiols in ambient aerosol in the southeastern United States. *Environ. Sci. Technol.* **2010**, *44*, 4590–4596.
- (44) Darer, A. I.; Cole-Filipiak, N. C.; O'Connor, A. E.; Elrod, M. J. Formation and stability of atmospherically relevant isoprene-derived organosulfates and organonitrates. *Environ. Sci. Technol.* **2011**, *45*, 1895–1902.
- (45) Liggio, J.; Li, S.-M.; McLaren, R. Reactive uptake of glyoxal by particulate matter. *J. Geophys. Res.* **2005**, *110*, D10304.
- (46) Volkamer, R.; Jimenez, J. L.; San Martini, F.; Dzepina, K.; Zhang, Q.; Salcedo, D.; Molina, L. T.; Worsnop, D. R.; Molina, M. J. Secondary organic aerosol formation from anthropogenic air pollution: Rapid and higher than expected. *Geophys. Res. Lett.* **2006**, *33*.
- (47) Heald, C. L.; et al. Exploring the vertical profile of atmospheric organic aerosol: Comparing 17 aircraft field campaigns with a global model. *Atmos. Chem. Phys.* **2011**, *11*, 12673–12696.
- (48) Ford, B.; Heald, C. L. Aerosol loading in the southeastern United States: Reconciling surface and satellite observations. *Atmos. Chem. Phys. Discuss.* **2013**, *13*, 9917–9952.
- (49) Fu, T.-M.; Jacob, D. J.; Wittrock, F.; Burrows, J. P.; Vrekoussis, M.; Henze, D. K. Global budgets of atmospheric glyoxal and methylglyoxal, and implications for formation of secondary organic aerosols. *J. Geophys. Res.* **2008**, *113*, D15303.
- (50) Offenberg, J. H.; Lewandowski, M.; Jaoui, M.; Kleindienst, T. E. Contributions of biogenic and anthropogenic hydrocarbons to secondary organic aerosol during 2006 in Research Triangle Park, NC. *Aerosol Air Qual. Res.* **2011**, *11*, 99–108.
- (51) Lin, L. I. A concordance correlation coefficient to evaluate reproducibility. *Biometrics* **1989**, *45*, 255–268.
- (52) Lin, L. I. A note on the concordance correlation coefficient. *Biometrics* **2000**, *56*, 324–325.
- (53) Cole-Filipiak, N. C.; O'Connor, A. E.; Elrod, M. J. Kinetics of the hydrolysis of atmospherically relevant isoprene-derived hydroxy epoxides. *Environ. Sci. Technol.* **2010**, *44*, 6718–6723.
- (54) Froyd, K. D.; Murphy, S. M.; Murphy, D. M.; de Gouw, J. A.; Eddingsaas, N. C.; Wennberg, P. O. Contribution of isoprene-derived organosulfates to free tropospheric aerosol mass. *Proc. Natl. Acad. Sci. U.S.A.* **2010**, *107*, 21360–21365.
- (55) Zhang, X.; Liu, Z.; Hecobian, A.; Zheng, M.; Frank, N. H.; Edgerton, S.; Weber, R. J. Spatial and seasonal variations of fine particle water-soluble organic carbon (WSOC) over the southeastern United States: implications for secondary organic aerosol formation. *Atmos. Chem. Phys.* **2012**, *12*, 6593–6607.
- (56) Piletic, I. R.; Offenberg, J. H.; Olson, D. A.; Jaoui, M.; Krug, J.; Lewandowski, M.; Turlington, J. M.; Kleindienst, T. E. Constraining carbonaceous aerosol sources in a receptor model using combined  $^{14}\text{C}$ , redox species, organic tracers, and elemental/organic carbon measurements. 2013, <http://dx.doi.org/10.1016/j.atmos-env.2013.07.062>.
- (57) Kleindienst, T. E.; Lewandowski, M.; Offenberg, J. H.; Edney, E. O.; Jaoui, M.; Zheng, M.; Ding, X. A.; Edgerton, E. S. Contribution of primary and secondary sources to organic aerosol and  $\text{PM}_{2.5}$  at SEARCH network sites. *J. Air Waste Manage. Assoc.* **2010**, *60*, 1388–1399.
- (58) Lewandowski, M.; Jaoui, M.; Kleindienst, T. E.; Offenberg, J. H.; Edney, E. O. Composition of  $\text{PM}_{2.5}$  during the summer of 2003 in Research Triangle Park, North Carolina. *Atmos. Environ.* **2007**, *41*, 4073–4083.
- (59) Ding, X.; Wang, X.; Xie, Z.; Zhang, Z.; Sun, L. Impacts of Siberian biomass burning on organic aerosols over the north Pacific Ocean and the Arctic: Primary and secondary organic tracers. *Environ. Sci. Technol.* **2013**, *47*, 3149–3157.
- (60) Henze, D. K.; Seinfeld, J. H.; Ng, N. L.; Kroll, J. H.; Fu, T. M.; Jacob, D. J.; Heald, C. L. Global modeling of secondary organic aerosol formation from aromatic hydrocarbons: High- vs. low-yield pathways. *Atmos. Chem. Phys.* **2008**, *8*, 2405–2420.
- (61) Ren, X. R.; et al. Behavior of OH and  $\text{HO}_2$  in the winter atmosphere in New York City. *Atmos. Environ.* **2006**, *40*, S252–S263.
- (62) Shilling, J. E.; Zaveri, R. A.; Fast, J. D.; Kleinman, L.; Alexander, M. L.; Canagaratna, M. R.; Fortner, E.; Hubbe, J. M.; Jayne, J. T.; Sedlacek, A.; Setyan, A.; Springston, S.; Worsnop, D. R.; Zhang, Q. Enhanced SOA formation from mixed anthropogenic and biogenic emissions during the CARES campaign. *Atmos. Chem. Phys.* **2013**, *13*, 2091–2113.
- (63) Lane, T. E.; Donahue, N. M.; Pandis, S. N. Effect of  $\text{NO}_x$  on secondary organic aerosol concentrations. *Environ. Sci. Technol.* **2008**, *42*, 6022–6027.
- (64) Carlton, A. G.; Pinder, R. W.; Bhawe, P. V.; Pouliot, G. A. To what extent can biogenic SOA be controlled? *Environ. Sci. Technol.* **2010**, *44*, 3376–3380.
- (65) Pye, H. O. T.; Chan, A. W. H.; Barkley, M. P.; Seinfeld, J. H. Global modeling of organic aerosol: The importance of reactive nitrogen ( $\text{NO}_x$  and  $\text{NO}_3$ ). *Atmos. Chem. Phys.* **2010**, *10*, 11261–11276.
- (66) Rollins, A. W.; Browne, E. C.; Min, K. E.; Pusede, S. E.; Wooldridge, P. J.; Gentner, D. R.; Goldstein, A. H.; Liu, S.; Day, D. A.; Russell, L. M.; Cohen, R. C. Evidence for  $\text{NO}_x$  control over nighttime SOA formation. *Science* **2012**, *337*, 1210–1212.
- (67) Bates, T. S.; Lamb, B. K.; Guenther, A.; Dignon, J.; Stoiber, R. E. Sulfur emissions to the atmosphere from natural sources. *J. Atmos. Chem.* **1992**, *14*, 315–337.
- (68) Tolocka, M. P.; Turpin, B. Contribution of organosulfur compounds to organic aerosol mass. *Environ. Sci. Technol.* **2012**, *46*, 7978–7983.